Astrocyte reactivity is associated with tau tangle load and cortical thinning in Alzheimer's disease

Tengfei Guo[1,2]* , Anqi Li[1], Pan Sun[1], Zhengbo He[1], Yue Cai[1], Guoyu Lan[1], Lin Liu[1], Jieyin Li[1], Jie Yang[1,3], Yalin Zhu[1], Ruiyue Zhao[4], Xuhui Chen[5], Dai Shi[6], Zhen Liu[1], Qingyong Wang[7], Linsen Xu[8], Liemin Zhou[6], Pengcheng Ran[9], Xinlu Wang[4], Kun Sun[10], Jie Lu[3,14]* and Ying Han[1,3,11,12,13]*

Abstract

Background It is not fully established whether plasma β-amyloid$(Aβ)_{42}/Aβ_{40}$ and phosphorylated Tau_{181} (p-Tau_{181}) can effectively detect Alzheimer's disease (AD) pathophysiology in older Chinese adults and how these biomarkers correlate with astrocyte reactivity, Aβ plaque deposition, tau tangle aggregation, and neurodegeneration.

Methods We recruited 470 older adults and analyzed plasma $Aβ_{42}/Aβ_{40}$, p-Tau_{181}, glial fibrillary acidic protein (GFAP), and neurofilament light (NfL) using the Simoa platform. Among them, 301, 195, and 70 underwent magnetic resonance imaging, Aβ and tau positron emission tomography imaging. The plasma $Aβ_{42}/Aβ_{40}$ and p-Tau_{181} thresholds were defined as ≤0.0609 and ≥2.418 based on the receiver operating characteristic curve analysis using the Youden index by comparing Aβ-PET negative cognitively unimpaired individuals and Aβ-PET positive cognitively impaired patients. To evaluate the feasibility of using plasma $Aβ_{42}/Aβ_{40}$ (A) and p-Tau_{181} (T) to detect AD and understand how astrocyte reactivity affects this process, we compared plasma GFAP, Aβ plaque, tau tangle, plasma NfL, hippocampal volume, and temporal-metaROI cortical thickness between different plasma A/T profiles and explored their relations with each other using general linear models, including age, sex, *APOE-ε4*, and diagnosis as covariates.

Results Plasma A+/T+ individuals showed the highest levels of astrocyte reactivity, Aβ plaque, tau tangle, and axonal degeneration, and the lowest hippocampal volume and temporal-metaROI cortical thickness. Lower plasma $Aβ_{42}/Aβ_{40}$ and higher plasma p-Tau_{181} were independently and synergistically correlated with higher plasma GFAP and Aβ plaque. Elevated plasma p-Tau_{181} and GFAP concentrations were directly and interactively associated with more tau tangle formation. Regarding neurodegeneration, higher plasma p-Tau_{181} and GFAP concentrations strongly correlated with more axonal degeneration, as measured by plasma NfL, and lower plasma $Aβ_{42}/Aβ_{40}$ and higher plasma p-Tau_{181} were related to greater hippocampal atrophy. Higher plasma GFAP levels were associated with thinner cortical

---

*Correspondence:
Tengfei Guo
tengfei.guo@szbl.ac.cn
Jie Lu
imaginglu@hotmail.com
Ying Han
hanying@xwh.ccmu.edu.cn
Full list of author information is available at the end of the article

thickness and significantly interacted with lower plasma $A\beta_{42}/A\beta_{40}$ and higher plasma p-Tau$_{181}$ in predicting more temporal-metaROI cortical thinning. Voxel-wise imaging analysis confirmed these findings.

Discussion This study provides a valuable reference for using plasma biomarkers to detect AD in the Chinese community population and offers novel insights into how astrocyte reactivity contributes to AD progression, highlighting the importance of targeting reactive astrogliosis to prevent AD.

Keywords Plasma biomarkers, Aβ, Tau, GFAP, Astrocyte reactivity, Alzheimer's disease

Background

Alzheimer's disease (AD) patients exhibit reduced concentrations of β-amyloid (Aβ)42($A\beta_{42}$) [1–3] in CSF or plasma and elevated cortical Aβ accumulation [4, 5]. This is followed by increased levels of phosphorylated Tau (p-Tau) in CSF or plasma [6] and cortical tau tangles [7, 8], ultimately leading to neurodegeneration and cognitive decline [9–11]. Recently, neuroinflammation has been strongly linked to AD progression, providing additional pathological insights to predict AD core pathologies and neurodegeneration [12]. Understanding the association between neuroinflammation, Aβ, tau, and neurodegeneration is critical for comprehending AD's characteristics and progression patterns.

Positron emission tomography (PET) imaging [9, 13] and CSF biomarkers [1, 6] are commonly used to detect abnormal alterations in AD pathologies. Previous studies using CSF biomarker [14, 15] and PET imaging [16–18] have demonstrated that individuals who are Aβ positive and tau positive (A+/T+) are at higher risk of AD than those who are Aβ negative and tau negative (A-/T-), Aβ positive and tau negative (A+/T-), and Aβ negative and tau positive (A-/T+). However, the high cost and limited availability of PET imaging and the invasiveness of lumbar puncture restrict their use in AD diagnosis. Advanced techniques for detecting plasma $A\beta_{42}/A\beta_{40}$ [19–21], p-Tau [22–28], astrocyte reactivity [29–31], and axonal degeneration [32, 33] suggest plasma biomarkers have great potential for diagnosing AD [34, 35].

Recently, plasma biomarker studies [36–40] and the latest NIA-AA research framework proposed by Jack and colleagues in AAIC suggest using a combination of plasma $A\beta_{42}/A\beta_{40}$ and plasma p-Tau, rather than each alone, to identify individuals at a high risk of AD. However, reliable thresholds for plasma $A_{\beta42}/A\beta_{40}$ and p-Tau$_{181}$ have not been established in older adults in the Chinese community. It remains unclear whether A+/T+individuals defined by plasma biomarkers have widespread cortical Aβ plaque, tau tangle, hippocampal atrophy, and cortical thinning compared to the plasma A-/T- individuals in a community-based aging cohort, particularly in China. Furthermore, plasma glial fibrillary acidic protein (GFAP) has emerged as a promising biomarker for representing astrocyte reactivity [30, 31, 41–43]. Recent studies [29, 44] have shown that plasma GFAP may affect the association between Aβ and tau. However, the associations among plasma $A\beta_{42}/A\beta_{40}$, plasma p-Tau$_{181}$, and plasma GFAP, as well as their independent and synergistic relationships to Aβ plaque accumulation, tau tangle aggregation, axonal degeneration, hippocampal atrophy, and AD-signature cortical thinning, remain unclear.

In this study, we analyzed plasma biomarkers, structural MRI, Aβ PET, and tau PET images based on a Chinese community-based aging cohort to (1) determine the effective thresholds for plasma $A\beta_{42}/A\beta_{40}$ and plasma p-Tau$_{181}$ in older Chinese adults and evaluate their feasibility for detecting the abnormal alternations in astrocyte reactivity, Aβ plaque, tau tangle, axonal degeneration, hippocampal atrophy, and cortical thinning; (2) and investigate the associations among plasma $A\beta_{42}/A\beta_{40}$, plasma p-Tau$_{181}$, and plasma GFAP, as well as how they independently and synergistically relate to Aβ plaque, tau tangle, axonal degeneration, hippocampal atrophy, and AD-signature cortical thinning in older adults. The ultimate goal of this study is to provide evidence of the feasibility of using plasma $A\beta_{42}/A\beta_{40}$ and plasma p-Tau$_{181}$ to identify individuals at high risk of AD in the community and to determine whether elevated plasma GFAP concentrations can further predict AD downstream events.

Methods

Participants

The community-based longitudinal cohort Greater-Bay-Area Healthy Aging Brain Study (GHABS) [45](clinicaltrials.gov ID: NCT06183658) was approved by the Shenzhen Bay Laboratory and collaborated hospitals' Ethical Committees, and was launched in May 2021. The written informed consent of the GHABS project was signed by each participant before enrollment. All the volunteer participants from the community in Guangdong-Hong Kong-Macao Greater-Bay-Area of South China underwent cognitive assessments, genetic screening, and blood sample collection, and part of them had MRI, Aβ PET, and tau PET scanning. The inclusion and exclusion criteria of the GHABS cohort were provided in the Supplementary Material. Participants were classified as cognitively unimpaired (CU), mild cognitive impairment (MCI), and AD dementia following the standard protocol of the ADNI cohort [46]. We analyzed 470 GHABS

participants who simultaneously completed cognitive assessments, plasma $A\beta_{42}/A\beta_{40}$, p-Tau$_{181}$, NfL, and GFAP data measured by the Simoa platform. Among them, 326, 87, and 57 were CU, MCI, and dementia. MCI and dementia patients were pooled as cognitively impaired (CI) individuals.

Plasma biomarkers and APOE genotyping

Participants fasted for one night the day before (not less than 6 h), and blood was drawn in the morning of the next day. The details of plasma sample processing can be found in *Supplementary Material*. The concentrations of $A\beta_{40}$, $A\beta_{42}$, NfL, GFAP, and p-Tau$_{181}$ in plasma were detected using commercial Simoa® NEUROLOGY 4-PLEX E (N4PE, cat: 103670), and pTau-181 (cat: 104111) in Simoa HD-X Analyzer™ (Quanterix Corp.) in Shenzhen Bay Laboratory. APOE genotype was determined by TaqMan™ SNP genotyping for the two single nucleotide polymorphisms (rs429358, rs7412) that detect the ε2, ε3, and ε4 alleles using the DNA Isolation Kit based on the blood cell by centrifuge from the EDTA blood sample.

MRI and PET imaging

All the MRI scanning sequences were conducted following the standard ADNI protocol. The 3 Plane Localizer positioning sequence and 3D T1 MPRAGE/IRSPGR MRI image data were collected on 3.0T scanners. The structural MRI images were segmented into different cortical and subcortical regions of interest (ROI) in Freesurfer (V7.2.0). The residual hippocampal volume (rHCV) was calculated using the hippocampal volume of both hemispheres and adjusted using the estimated total intracranial volume as we described previously [9]. In addition, the cortical thickness of AD-signature atrophy brain regions was obtained by calculating the surface area-weighted average thickness of the bilateral entorhinal, fusiform, inferior temporal, and middle temporal cortices [47].

The Aβ PET radiotracer [18F]D3FSP (FSP) [48] and tau PET radiotracer [18F]-flortaucipir (FTP) [49] were used for Aβ PET and tau PET imaging respectively. The Aβ PET and tau PET data acquisition were performed on a GE Discovery™ MI Gen 2 PET/CT scanner and a Siemens Biograph™ TruePoint™ PET/CT scanner. The spatial resolution of each PET scanner was quantified with PET imaging of a Hoffman phantom. For the Aβ PET imaging, the participants were injected with [18F]-D3FSP intravenously at 370 MBq (10 mCi±10%), rested for 45 min, and prepared for the scanning. [18F]-D3FSP Aβ PET/CT imaging was performed 50 min after injection, and the PET acquisition time was 20 min. For the tau PET imaging, the participants were injected with [18F]-flortaucipir intravenously at 370 MBq (10 mCi±10%), rested for

75 min, and prepared for imaging. The dynamic acquisition of [18F]-flortaucipir tau PET data was completed 80–100 min after the radiotracer administration.

The PET and MRI images were processed using in-house Matlab algorithms. The PET images were co-registered with their corresponding structural MRI images in SPM12 (Statistical Parametric Mapping). Sixty-eight Freesurfer-defined cortical ROIs obtained from MRI segmentation were used to extract regional FSP and FTP measurements from the co-registered PET images. The FSP SUVR of AD summary cortical regions (posterior cingulate cortex, precuneus, frontal lobe, parietal lobe, and lateral temporal) was obtained by dividing the radiotracer uptake value of AD typical brain regions by that in the brainstem. The FTP SUVR of the AD temporal-meta-ROI [47] (entorhinal cortex, parahippocampal gyrus, amygdala, inferior temporal and middle temporal brain regions) was used to evaluate cortical tau deposition. For voxel-wise analysis, FSP and FTP SUVR images were intensity-normalized and spatially-normalized at the voxel-wise level in the MNI space in SPM12 (Welcome Department of Imaging Neuroscience, London, UK) as we described previously [8].

Thresholds of FSP Aβ PET, plasma $A\beta_{42}/A\beta_{40}$, and plasma p-Tau$_{181}$

The bimodal distribution of COMPOSITE FSP SUVRs (Supplemental Fig. 1) enables us to use the Gaussian mixed model to estimate two Gaussian distributions of low Aβ and high Aβ to define an unsupervised threshold as COMPOSITE FSP SUVR≥0.76 (Supplemental Fig. 1), which corresponds to a 90% probability of belonging to the high Aβ distribution. The plasma $A\beta_{42}/A\beta_{40}$ ratio and plasma p-Tau$_{181}$ did not have clear bimodal distributions. Thus, we defined their thresholds by classifying Aβ PET negative CU individuals and Aβ PET positive CI individuals in the receiver operating characteristic (ROC) curve analysis using the Youden index. The cutoff ≤ 0.0609 for plasma $A\beta_{42}/A\beta_{40}$ ratio was defined as the optimal threshold for classifying 154 Aβ- CU participants and 69 Aβ+CI individuals in the ROC curve analysis (Supplemental Figs. 2–3). Similarly, the ROC analysis classified 143 Aβ- CU participants and 67 Aβ+CI participants as the endpoint to define the cutoff ≥ 2.418 for plasma p-Tau$_{181}$ (Supplemental Figs. 4–5). The thresholds of plasma $A\beta_{42}/A\beta_{40}$ ratio and plasma p-Tau$_{181}$ divided the whole cohort into 4 different plasma staging profiles: A-/T-, A-/T+, A+/T-, and A+/T+groups.

Statistical analysis

All the statistical analyses were done using R (v4.3.0, The R Foundation for Statistical Computing). The normal distribution of the data in this study was determined using the Shapiro-Wilk test. We used a two-tailed

Mann-Whitney U test and Fisher's exact test to compare the continuous and categorical characteristics at baseline between different A/T groups, respectively. Data were presented as median (interquartile range, IQR) or No. (%) unless otherwise noted.

Plasma p-Tau$_{181}$, plasma GFAP, and plasma NfL were log$_{10}$ transferred before the following analysis to meet the normal distribution. Generalized linear models (GLM) were used to compare plasma GFAP, COMPOSITE FSP Aβ SUVR, temporal-metaROI FTP SUVR, plasma NfL, rHCV, and temporal-metaROI cortical thickness between different A/T (A: plasma Aβ$_{42}$/Aβ$_{40}$, T: plasma p-Tau$_{181}$) groups, controlling for age, sex, *APOE-ε4*, and diagnosis:

$$Biomarkers \sim plasma\ A/T\ profiles\ + \\ age\ +\ sex + APOE - \varepsilon 4\ +\ diagnosis \tag{1}$$

Subsequently, we used GLM models to explore the association of plasma GFAP with plasma Aβ$_{42}$/Aβ$_{40}$ and plasma p-Tau$_{181}$, including the same covariates above:

$$Plasma\ GFAP \sim plasma\ A\beta_{42}/A\beta_{40} \times \\ plasma\ p - Tau_{181}\ +\ covariates \tag{2}$$

Besides, we investigated the association of plasma GFAP with plasma NfL, FSP SUVR, FTP SUVR, rHCV, and temporal-metaROI cortical thickness, including the same covariates above as well as without (model 3) and with (model 4), including plasma Aβ$_{42}$/Aβ$_{40}$ and plasma p-Tau$_{181}$ in the model:

$$Biomarkers \sim plasma\ GFAP\ +\ covariates \tag{3}$$

$$Biomarkers \sim plasma\ GFAP\ +\ plasma\ A\beta_{42}/A\beta_{40} + \\ plasma\ p - Tau_{181}\ +\ covariates \tag{4}$$

Furthermore, we investigated the independent and synergistic effect of plasma Aβ$_{42}$/Aβ$_{40}$, plasma p-Tau$_{181}$, and plasma GFAP with plasma NfL, FSP SUVR, FTP SUVR, rHCV, and temporal-metaROI cortical thickness, including the same covariates above:

$$Biomarkers \sim plasma A\beta_{42}/A\beta_{40} \times plasma\ p- \\ Tau_{181} \times plasma\ GFAP\ +\ covariates \tag{5}$$

Notably, all the statistic in these models were obtained based on the continuous variables in order to avoid any influences from the pre-defined thresholds. To better illustrate the association of plasma GFAP with plasma Aβ$_{42}$/Aβ$_{40}$ and plasma p-Tau$_{181}$, as well as how plasma GFAP modulates the association of plasma Aβ$_{42}$/Aβ$_{40}$ and plasma p-Tau$_{181}$ with FSP SUVR, FTP SUVR, plasma NfL, rHCV, and temporal-metaROI cortical thickness,

we plotted the association in the analysis of models (2) and (5) above in individuals with high (>Median) and low (<Median) plasma Aβ$_{42}$/Aβ$_{40}$, plasma p-Tau$_{181}$, and plasma GFAP separately. The *Pearson* correlation test calculated the correlation coefficient *R* between outcome and predictor in individuals with high (>Median) and low (<Median) plasma Aβ$_{42}$/Aβ$_{40}$, plasma p-Tau$_{181}$, and plasma GFAP.

Subsequently, we investigated the voxel-wise association between plasma Aβ$_{42}$/Aβ$_{40}$ and FSP Aβ PET images in all the participants with FSP Aβ PET images, participants with high (>Median) and low (<Median) plasma p-Tau$_{181}$ concentrations separately, controlling for the same covariates above. Furthermore, we studied the voxel-wise association of FTP tau PET images with plasma p-Tau$_{181}$ in all the individuals, individuals with high (>Median) and low (<Median) plasma GFAP concentrations separately, including the same covariates above. The voxel-wise associations between plasma Aβ$_{42}$/Aβ$_{40}$ and FSP Aβ PET images and between plasma p-Tau$_{181}$ and FTP tau PET images were presented using an uncorrected voxel threshold of $p < 0.001$, and the T-maps were converted into R-maps using the CAT12 toolbox (www.neuro.uni-jena.de/cat/) and displayed with family-wise error (FWE) corrected $p < 0.05$.

To evaluate how plasma GFAP modulates the voxel-wise association of cortical thickness images with plasma Aβ$_{42}$/Aβ$_{40}$ and plasma p-Tau$_{181}$, we resampled the cortical thickness images, mapped them to the fsaverage space and smoothed with a kernel size of 10 mm full-width at half maximum. We finally determined the vertex-wise association of the cortical thickness images with plasma Aβ$_{42}$/Aβ$_{40}$ and plasma p-Tau$_{181}$, controlling for the same covariates above. We did the vertex-wise analysis in all the participants with MRI data, participants with high (>Median) and low (<Median) plasma GFAP concentrations separately. The vertex-wise association between cortical thickness images and plasma p-Tau$_{181}$ was presented using an uncorrected voxel threshold of $p < 0.001$ (Monte Carlo simulation corrected for multiple comparisons) with FWE corrected $p < 0.05$ at the cluster level, and the statistical results were overlaid onto inflated cortical surfaces. For plasma Aβ$_{42}$/Aβ$_{40}$, we only showed the results of an uncorrected voxel threshold of $p < 0.001$ because no significant cluster survived after correction.

Results

Demographics of participants

The demographic characteristics of participants at baseline are summarized in Table 1. At baseline, A+/T+individuals had older ages, higher percentages of *APOE-ε4* carriers, and lower MoCa and MMSE scores than A-/T-individuals. The A+/T+group also had higher percentages of *APOE-ε4* carriers and lower MoCa and MMSE

Table 1 Demographics of participants included in this study

	A-/T-	A-/T+	A+/T-	A+T+
No., %	206, 43.8%	60, 12.8%	121, 25.7%	83, 17.7%
CI (No., %)	27, 22.1%	23, 38.3%	35, 28.9%	59, 71.1%
Age, years	65 (8.7,56–86)	[a]69 (11.2,55–86)	[a]67 (8.8,55–85)	[a, b]72 (9.9,56–89)
APOE-ε4 (No., %)	35, 17.0%	[a]18, 30.0%	27, 22.3%	[a, b, c]42, 50.6%
Female (No., %)	142, 68.9%	33, 55.0%	84, 69.4%	46, 55.4%
MoCa	26.0 (4.0)	[a]25.0 (5.25)	26.0 (5.0)	[a, b, c]16.0 (12.5)
MMSE	29.0 (3.0)	[a]28.0 (4.0)	[a]280 (3.0.)	[a, b, c]24.0 (10.0.)
Participants with MRI image data (_n_ = 301)				
No., %	122, 40.5%	43, 14.3%	74, 24.6%	62, 20.6%
CI (No., %)	18, 14.8%	14, 32.6%	22, 29.7%	42, 67.7%
Age, years	66 (7.4,56–81)	68 (10.7,55–86)	67 (8.3,55–83)	[a, b]72 (10.1,56–89)
APOE-ε4 (No., %)	27, 22.1%	10, 23.3%	15, 20.3%	[a, b, c]33, 53.2%
Female (No., %)	81, 66.4%	24, 55.8%	52, 70.3%	36, 58.1%
MoCa	26.0 (3.75)	[a]25. (5.5)	26.0 (5.0)	[a, b, c]19.0 (12.75)
MMSE	29.0 (3.0.)	[a]28.0 (4.0)	[a]28.0 (3.0)	[a, b, c]24.0 (10.75)
Participants with Aβ PET image data (_n_ = 195)				
No., %	78, 40.0%	30, 15.4%	41, 21.0%	46, 23.6%
CI (No., %)	13,16.7%	12, 40%	15, 36.6%	32, 69.6%
Age, years	66 (8.6,55–89)	67 (7.4,55–81)	[a, b]69 (9.1,58–89)	[a, b]73 (12.7,58–85)
APOE-ε4 (No., %)	18, 23.1%	7, 23.3%	[b]8, 19.5%	[a, b, c]25, 54.3%
Female (No., %)	48, 61.5%	16, 53.3%	28, 68.3%	25, 54.3%
MoCa	26.0 (3.0)	[c]25.0 (6.0)	26.0 (4.0)	[a, b, c]20.0. (12.0)
MMSE	29.0 (3.0)	[a]27.0 (4.75)	[a]27.0 (30)	[a, b, c]24.0 (9.75)
Participants with tau PET image data (_n_ = 70)				
No., %	16, 22.9%	10, 14.3%	18, 25.7%	26, 37.1%
CI (No., %)	4, 25.0%	4, 40.0%	5, 27.8%	16, 61.5%
Age, years	64(7.1.7,57–77)	65(8.2,58–77)	66(8.7,55–83)	[a]71(12.7,56–89)
APOE-ε4 (No., %)	9, 56.3%	4, 40.0%	6, 33.3%	17, 65.4%
Female (No., %)	8, 50.0%	5, 50.0%	12, 66.7%	15, 57.8%
MoCa	28.0 (2.5)	25.5 (7.0)	[a]24.5 (4.0)	[a, b, c]18.5 (11.75)
MMSE	29.0 (1.25)	27.0 (2.5)	[b]27.5 (2.75)	[a, b, c]24 (9.75)

Note: [a, b,c] indicate significantly different from A-/T-, A+/T-, and A-/T+ groups respectively

scores than the A-/T+and A+/T- groups. Moreover, 301, 195, and 70 individuals had concurrent MRI, ^{18}F-D3-FSP Aβ PET, and FTP tau PET scans.

Comparisons of plasma biomarkers and neuroimages among different A/T stages

Regarding the comparisons of different A/T profiles defined by plasma $A\beta_{42}/A\beta_{40}$ (A) and plasma p-Tau$_{181}$ (T), we found that A+T+individuals showed higher plasma GFAP, COMPOSITE Aβ PET SUVR, temporal-metaROI FTP SUVR, and lower rHCV, and temporal-metaROI cortical thickness than A-/T-, A-/T+, and A+/T- groups (Fig. 1A, C-F). Besides, A+T+individuals only had higher plasma NfL than A-/T-group (Fig. 1B). The *Supplemental Material* provided more details on the comparisons between the A+/T+group and other groups.

Furthermore, A-/T+individuals had higher plasma NfL concentrations than A+/T- group (standardized β (β_{std})=0.316[95% confidence interval (ci), 0.069, 0.563], Fig. 1B), and higher COMPOSITE Aβ PET SUVR than A-/T- group (β_{std}=0.462[95% ci, 0.153, 0.770], Fig. 1C). In addition, A+/T- individuals showed higher plasma GFAP concentrations than A-/T- group (β_{std}=0.253[95% ci, 0.063, 0.443], Fig. 1A) and A-/T+ (β_{std}=0.303[95% ci, 0.041, 0.565], Fig. 1A) group.

Association of plasma $A\beta_{42}/A\beta_{40}$, p-Tau$_{181}$, GFAP and NfL

For the astrocyte reactivity measured by plasma GFAP, we found lower plasma $A\beta_{42}/A\beta_{40}$ (Fig. 2B, β_{std} = -0.320[95% ci, -0.397, -0.244], $p<0.001$), higher plasma p-Tau$_{181}$ (Fig. 2C, β_{std}=0.203[95% ci, 0.117, 0.288], $p<0.001$), older ages (β_{std}=0.289[95% ci, 0.211, 0.367], $p<0.001$), and females (β_{std}=0.320[95% ci, 0.167, 0.473], $p<0.001$) were related to higher plasma GFAP levels. Lower plasma $A\beta_{42}/A\beta_{40}$ and higher plasma p-Tau$_{181}$ concentrations showed significant interaction (Fig. 2A, β_{std} = -0.130[95% ci, -0.205, -0.055], $p<0.001$) with higher plasma GFAP levels. Specifically, the negative association between plasma $A\beta_{42}/A\beta_{40}$ and plasma GFAP was marginally stronger (Fig. 2D, β_{std} = -0.145[95% ci, -0.297, 0.007], $p=0.061$) among individuals with high (>median) plasma p-Tau$_{181}$ concentrations than those with low plasma p-Tau$_{181}$ concentrations. The positive association between plasma p-Tau$_{181}$ and plasma GFAP was more robust (Fig. 2E, β_{std}=0.281[95% ci, 0.123, 0.439], $p<0.001$) in individuals with low (<median) plasma $A\beta_{42}/A\beta_{40}$ than that in individuals with high (>median) plasma $A\beta_{42}/A\beta_{40}$.

We further determined the association of plasma $A\beta_{42}/A\beta_{40}$, plasma p-Tau$_{181}$, and plasma GFAP with plasma NfL. No significant interaction was found between plasma $A\beta_{42}/A\beta_{40}$, plasma p-Tau$_{181}$, and plasma GFAP in predicting the levels of plasma NfL, although higher
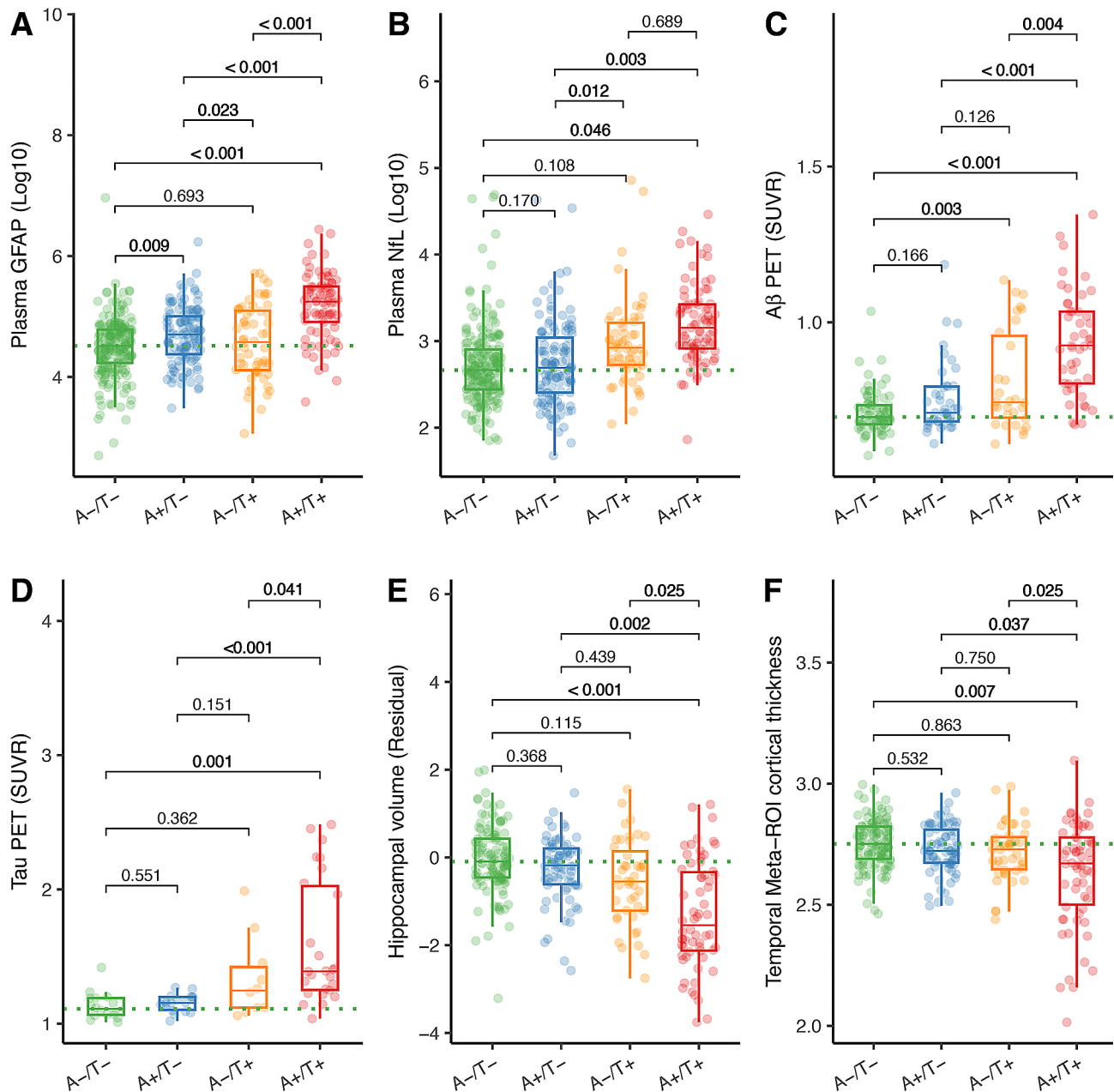
Fig. 1 Comparisons of plasma biomarkers and neuroimaging between different A/T profiles. Comparisons of **(A)** plasma GFAP, **(B)** plasma NfL, **(C)** Aβ PET, **(D)** tau PET, **(F)** residual hippocampal volume (rHCV), and **(G)** temporal-MetaROI cortical thickness between A-/T-, A+/T-, A-/T+, and A+/T+ groups. Plasma GFAP and plasma NfL were $\log_{10}$ transferred before they were used in the general linear models. For the boxplots, each point represents an individual, and the dashed lines represent the median values of the A-/T- group. The median (horizontal bar), interquartile range (IQR, hinges), and $1.5 \times$ IQR (whiskers) were presented in boxplots as well. The *p* values of the comparisons were shown at the top, adjusting for age, sex, *APOE-ε4* status, and diagnosis
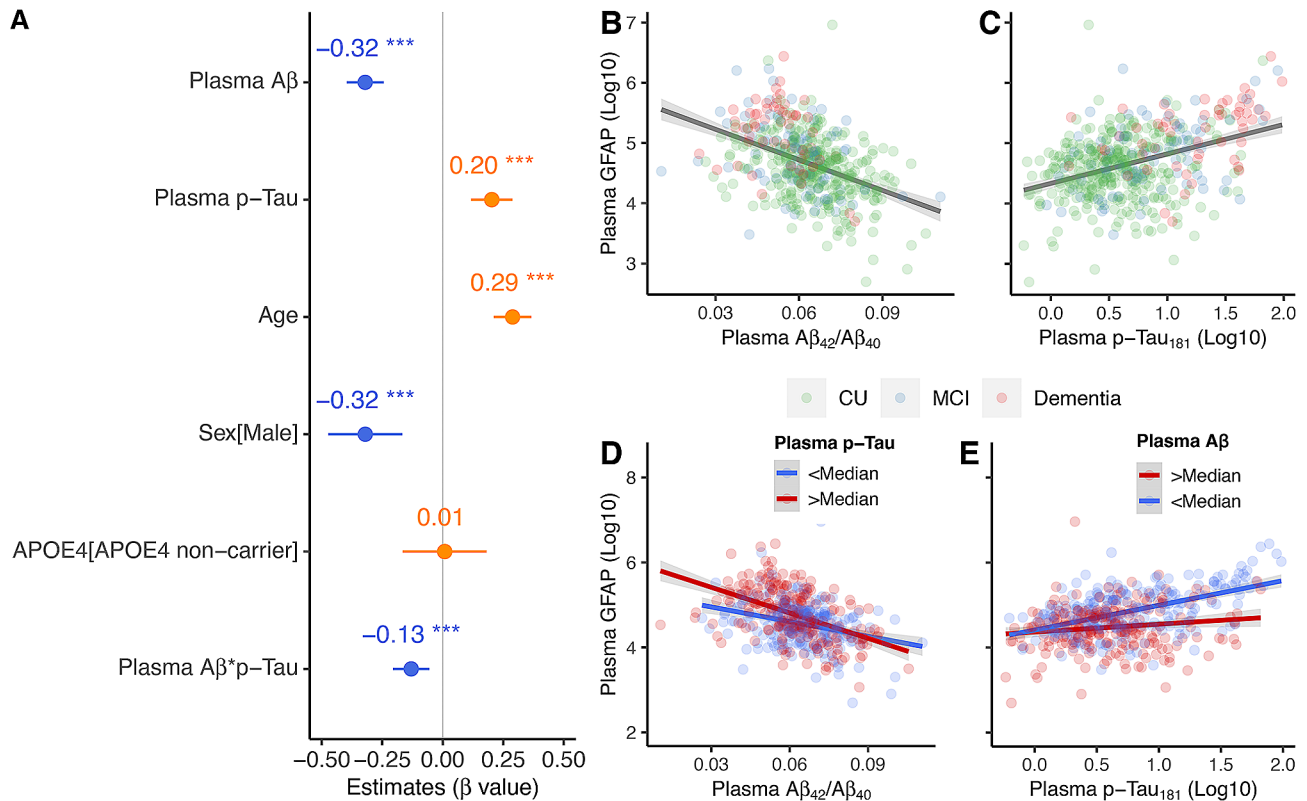
plasma p-Tau$_{181}$ and plasma GFAP concentrations, older ages, and males were associated with higher plasma NfL levels (Supplemental Fig. 6).

Association of plasma Aβ$_{42}$/Aβ$_{40}$, p-Tau$_{181}$, and GFAP with Aβ plaques and tau tangles

Regarding the association of plasma GFAP, plasma Aβ$_{42}$/Aβ$_{40}$ and plasma p-Tau$_{181}$ with Aβ PET and tau PET, we found that plasma GFAP was related to higher Aβ PET

regardless of including plasma Aβ$_{42}$/Aβ$_{40}$ and plasma p-Tau$_{181}$ as the covariates (Supplemental Fig. 7, before including covariates: $\beta_{std}=0.300$[95% ci, 0.181, 0.419], $p<0.001$; after including covariates: $\beta_{std}=0.152$[95% ci, 0.032, 0.273], $p=0.022$) and tau PET ($\beta_{std}=0.470$[95% ci, 0.288, 0.651], $p<0.001$; $\beta_{std}=0.335$[95% ci, 0.139, 0.461], $p<0.001$).

Subsequently, we investigated the independent and synergistic predictive effect of plasma Aβ$_{42}$/Aβ$_{40}$,

Fig. 2 Association of plasma $A\beta_{42}/A\beta_{40}$ and plasma p-Tau$_{181}$ with plasma GFAP. Association of plasma $A\beta_{42}/A\beta_{40}$ and plasma p-Tau$_{181}$ with plasma GFAP **(A-C)**. For better illustration, the association of plasma GFAP with plasma $A\beta_{42}/A\beta_{40}$ and plasma p-Tau$_{181}$ were presented in different subgroups (< Median and > Median) of **(D)** plasma p-Tau$_{181}$ and **(E)** plasma $A\beta_{42}/A\beta_{40}$, but the interactive effect on plasma GFAP of plasma $A\beta_{42}/A\beta_{40}$ and plasma p-Tau$_{181}$ were conducted using continuous variables. Plasma p-Tau$_{181}$ and plasma GFAP were $\log_{10}$ transferred before they were used in the general linear models

p-Tau$_{181}$, and GFAP at cortical Aβ plaques and tau tangles. Lower plasma $A\beta_{42}/A\beta_{40}$ (β_{std} = -0.210[95% ci, -0.324, -0.097], $p<0.001$), higher plasma p-Tau$_{181}$ concentrations (β_{std}=0.351[95% ci, 0.226, 0.475], $p<0.001$), and *APOE-ε4* carriers (β_{std}=0.341[95% ci, 0.123, 0.558], $p=0.002$) were associated with higher Aβ PET SUVR (Fig. 3A-C), whereas the relation between plasma GFAP and Aβ PET SUVR became marginal (β_{std}=0.120[95% ci, -0.007, 0.247], $p=0.064$). Moreover, the negative association between plasma $A\beta_{42}/A\beta_{40}$ and Aβ PET SUVR was stronger in individuals with high (>median) plasma p-Tau$_{181}$ concentrations (R = -0.52[95% ci, -0.651, -0.358], $p<0.001$) than those with low (<median) plasma p-Tau$_{181}$ concentrations (R =-0.19[95% ci, -0.371, 0.014], $p=0.069$) (Fig. 3D). In contrast, higher plasma p-Tau$_{181}$ (Fig. 3F, β_{std}=0.278[95% ci, 0.117, 0.439], $p<0.001$) and plasma GFAP (Fig. 3G, β_{std}=0.244[95% ci, 0.047, 0.441], $p=0.015$) concentrations but not plasma $A\beta_{42}/A\beta_{40}$ were associated with higher temporal-metaROI tau PET SUVR. Notably, plasma p-Tau$_{181}$ and plasma GFAP showed significant interactive relation (Fig. 3E, β_{std}=0.221[95% ci, 0.101, 0.342], $p<0.001$) with higher tau PET SUVR. Specifically, the positive association between plasma p-Tau$_{181}$ and tau PET SUVR was more robust (Fig. 3H) in individuals

with high (>median) plasma GFAP concentrations (R=0.71[95% ci, 0.488, 0.842], $p<0.001$) than in individuals with low (<median) plasma GFAP concentrations (R=0.41[95% ci, 0.088, 0.653], $p=0.015$).

The voxel-wise analysis was consistent with the ROI analysis, where we found plasma $A\beta_{42}/A\beta_{40}$ and Aβ PET SUVR showed significant negative association in the whole cohort and individuals with high (>median) plasma p-Tau$_{181}$ concentrations but not in individuals with low (<median) plasma p-Tau$_{181}$ concentrations (Fig. 4A-C). The voxel-wise analysis between plasma p-Tau$_{181}$ and FTP tau PET images replicated the ROI analysis findings (Fig. 4D-F).
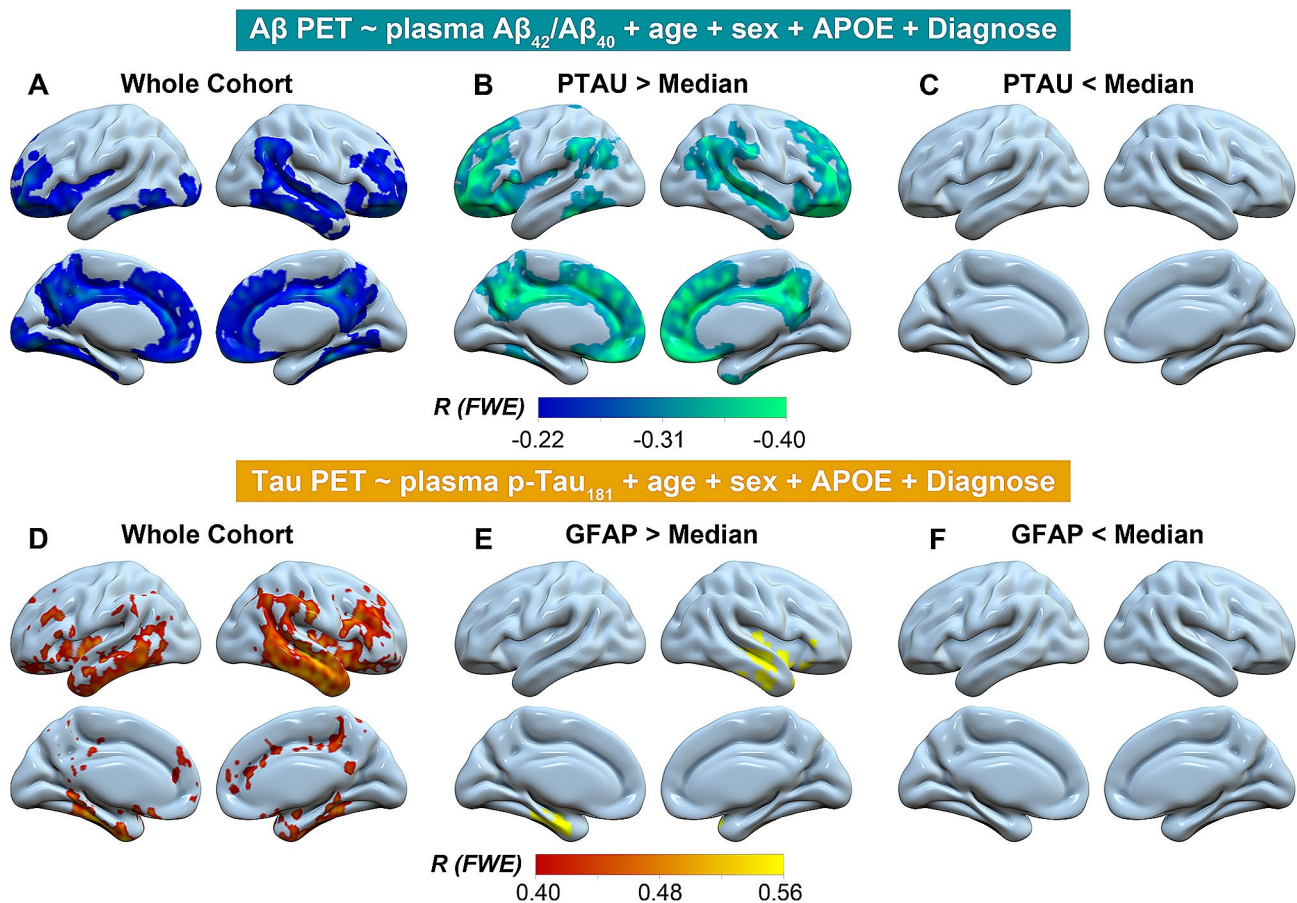
Association of plasma $A\beta_{42}/A\beta_{40}$, p-Tau$_{181}$, and GFAP with hippocampal atrophy and cortical thinning

Regarding the hippocampal atrophy and AD-signature cortical thinning, higher plasma GFAP concentrations were associated with more hippocampal atrophy (β_{std} = -0.146[95% ci, -0.246, -0.047], $p=0.004$) before controlling for plasma $A\beta_{42}/A\beta_{40}$ and plasma p-Tau$_{181}$, whereas the relation disappeared (β_{std} = -0.066[95% ci, -0.171, 0.039], $p=0.218$) after including them as the covariates in the model (Supplemental Fig. 8A-B). In contrast, elevated
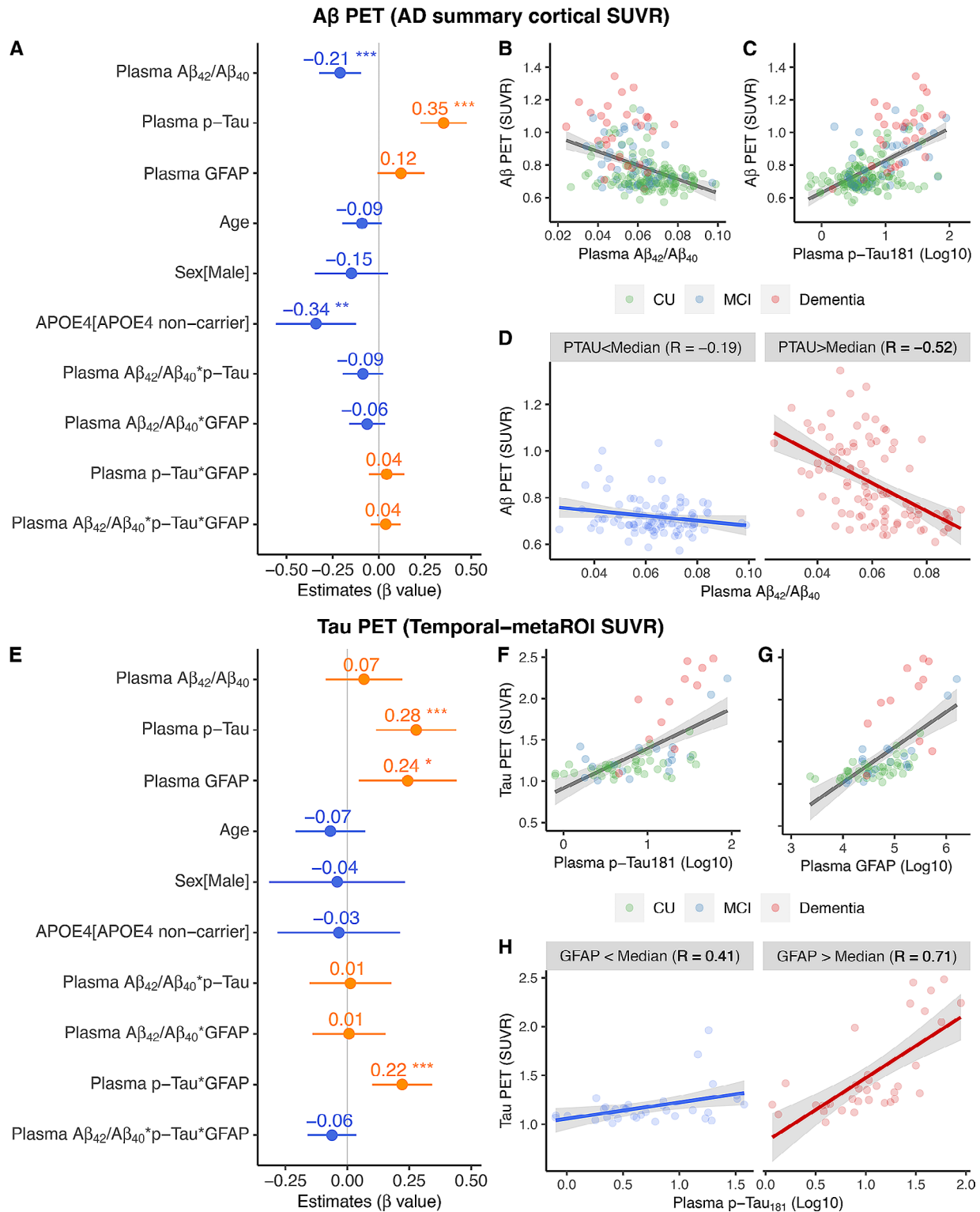
Fig. 3 Association of plasma $A\beta_{42}/A\beta_{40}$, plasma p-Tau$_{181}$, and plasma GFAP with $A\beta$ PET and tau PET. Association of plasma $A\beta_{42}/A\beta_{40}$, plasma p-Tau$_{181}$, and plasma GFAP with **(A-C)** $A\beta$ PET and **(E-G)** tau PET. Notably, plasma p-Tau$_{181}$ and plasma GFAP were log_{10} transferred before they were used in the general linear models. Notably, the interactive effects on $A\beta$ PET and tau PET of plasma $A\beta_{42}/A\beta_{40}$, plasma p-Tau$_{181}$, and plasma GFAP were conducted using continuous variables. For better illustration, **(D)** the association between $A\beta$ PET and plasma $A\beta_{42}/A\beta_{40}$ was presented in different subgroups (< Median and > Median) of plasma p-Tau$_{181}$, and **(H)** the association between tau PET and plasma p-Tau$_{181}$ was presented in different subgroups (< Median and > Median) of plasma GFAP.

Fig. 4 Voxel-wise association of plasma $A\beta_{42}/A\beta_{40}$, plasma p-Tau$_{181}$ with $A\beta$ PET and tau PET. Voxel-wise association of plasma $A\beta_{42}/A\beta_{40}$ and plasma p-Tau$_{181}$ with **(A-C)** $A\beta$ PET and **(D-F)** tau PET in the whole cohort, individuals with plasma p-Tau$_{181}$ or plasma GFAP > Median and < Median. Notably, Plasma p-Tau$_{181}$ and plasma GFAP were $\log_{10}$ transferred before they were used in the general linear models

plasma GFAP levels were correlated with more temporal-metaROI cortical thinning regardless of controlling for plasma $A\beta_{42}/A\beta_{40}$ and plasma p-Tau$_{181}$ (Supplemental Fig. 8C-D, before including covariates: β_{std} = -0.210[95% ci, -0.322, -0.098], $p<0.001$; after including covariates: β_{std} = -0.176[95% ci, -0.297, -0.054], $p=0.011$).

In models aiming to investigate the independent and interactive effect of plasma GFAP, plasma $A\beta_{42}/A\beta_{40}$, and plasma p-Tau$_{181}$ on hippocampal atrophy and AD-signature cortical thinning, we found higher plasma GFAP concentrations (β_{std} = -0.162[95% ci, -0.288, -0.035], $p=0.012$) and *APOE-ε4* non-carriers (β_{std} = -0.363[95% ci, -0.586, -0.141], $p=0.001$) were related to more shrinking in temporal-metaROI cortical thickness (Fig. 5A). Additionally, plasma GFAP showed significant interaction with plasma $A\beta_{42}/A\beta_{40}$ (β_{std}=0.113[95% ci, 0.004, 0.223], $p=0.042$) and plasma p-Tau$_{181}$ (β_{std} = -0.200[95% ci, -0.296, -0.104], $p<0.001$) at predicting temporal-metaROI cortical thinning. To be more specific, the associations of plasma $A\beta_{42}/A\beta_{40}$ and plasma p-Tau$_{181}$ with temporal-metaROI cortical thickness were more robust in individuals with high (>median) plasma

GFAP concentrations (plasma $A\beta_{42}/A\beta_{40}$: $R=0.21$[95% ci, 0.051, 0.357], $p=0.010$; plasma p-Tau$_{181}$: R = -0.37[95% ci, -0.497, -0.219], $p<0.001$) than in individuals with low (<median) plasma GFAP concentrations (plasma $A\beta_{42}/A\beta_{40}$: $R=0.08$[95% ci, -0.081, 0.238], $p=0.326$; plasma p-Tau$_{181}$: $R=0.01$[95% ci, -0.149, 0.171], $p=0.893$) (Fig. 5B-C). The vertex-wise analysis of cortical thickness images with plasma $A\beta_{42}/A\beta_{40}$ and plasma p-Tau$_{181}$ substantially replicated the ROI analysis findings (Fig. 6A-F). In contrast, we did not find interaction in any biomarkers on hippocampal atrophy, although we observed that lower plasma $A\beta_{42}/A\beta_{40}$ (β_{std}=0.117[95% ci, 0.015, 0.218], $p=0.024$), higher plasma p-Tau$_{181}$ concentrations (β_{std} = -0.190[95% ci, -0.306, -0.075], $p=0.001$), and older ages (β_{std} = -0.274[95% ci, -0.371, -0.176], $p<0.001$) but not plasma GFAP concentrations were related to more decreases in rHCV (Supplemental Fig. 9).

Discussion

In this study, we established the thresholds for plasma $A\beta_{42}/A\beta_{40}$ and plasma p-Tau$_{181}$ and demonstrated that individuals positive for these biomarkers (A+/T+)
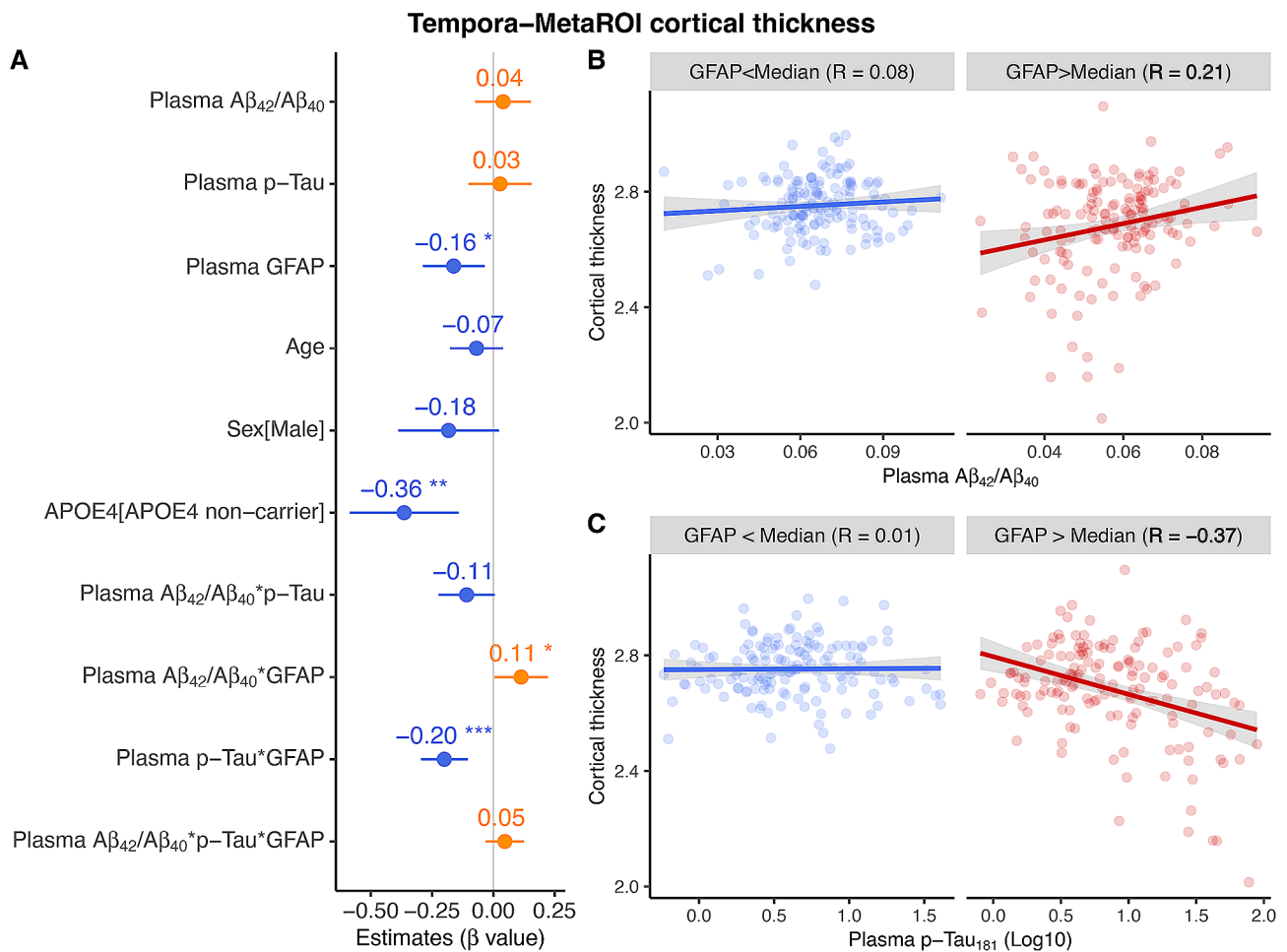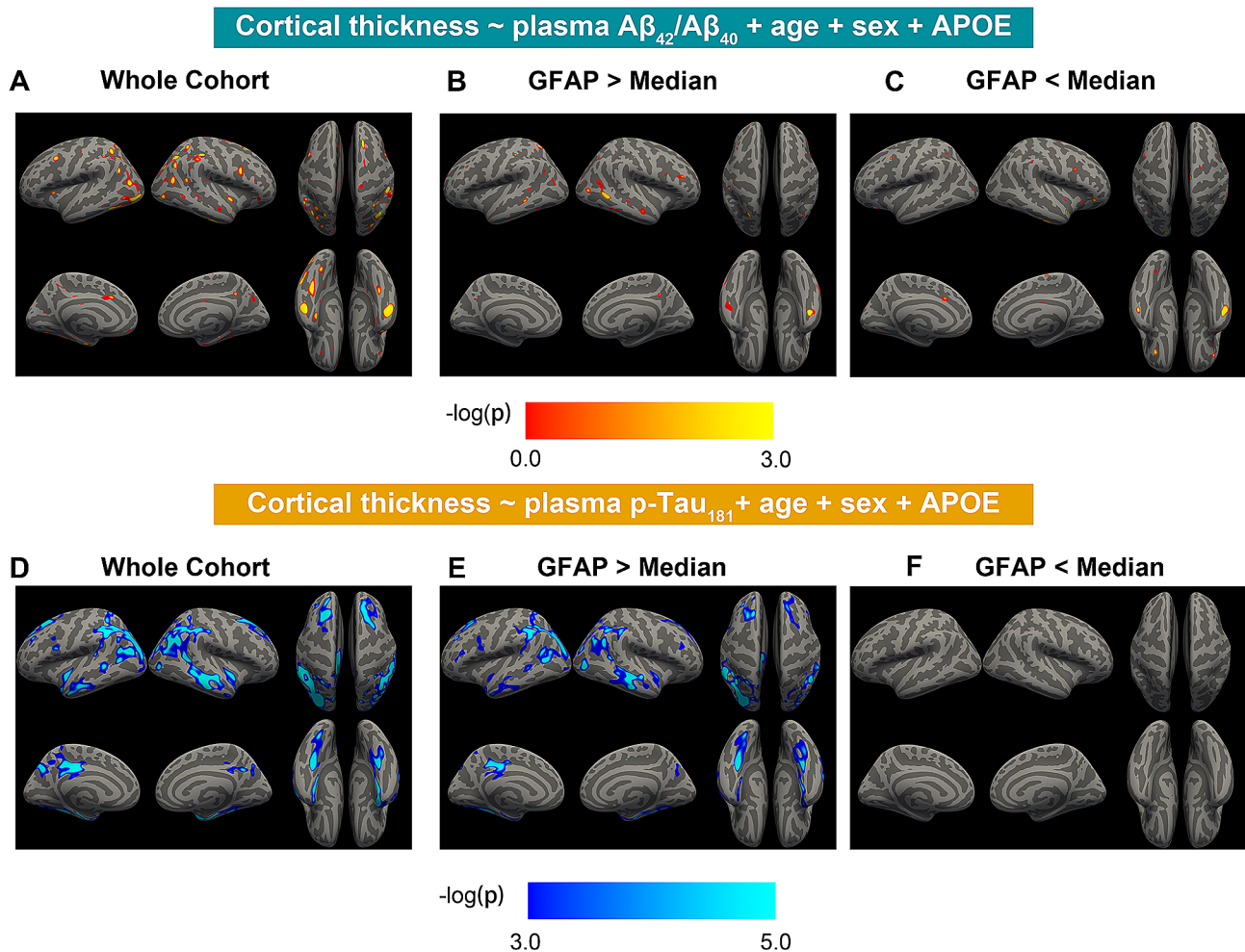
Fig. 5 Association of plasma $A\beta_{42}/A\beta_{40}$, plasma p-Tau$_{181}$, and plasma GFAP with cortical thinning. Association of plasma $A\beta_{42}/A\beta_{40}$, plasma p-Tau$_{181}$, and plasma GFAP with **(A)** temporal-metaROI cortical thickness. Notably, Plasma p-Tau$_{181}$ and plasma GFAP were log$_{10}$ transferred before they were used in the general linear models. Notably, the interactive effect of plasma $A\beta_{42}/A\beta_{40}$ and plasma p-Tau$_{181}$ with plasma GFAP on temporal-metaROI cortical thinning were conducted using continuous variables. For better illustration, the association of temporal-metaROI cortical thickness with **(B)** plasma $A\beta_{42}/A\beta_{40}$ and **(C)** plasma p-Tau$_{181}$ was presented in different subgroups (< Median and > Median) of plasma GFAP

exhibited the most significant alterations in plasma GFAP, $A\beta$ PET, tau PET, plasma NfL, hippocampal volume, and AD-signature cortical thickness within a Chinese community-based aging cohort. Higher astrocyte reactivity, as measured by plasma GFAP, was strongly linked with tau tangle aggregation and cortical thickness thinning in AD. Importantly, the thresholds of plasma $A\beta_{42}/A\beta_{40}$ and plasma p-Tau$_{181}$ reported in this study are significant references for detecting AD in the older Chinese Han community population. These findings provide novel insights into the association among $A\beta$, tau, astrocyte reactivity, and neurodegeneration in AD.

Currently, there are no definitive thresholds for AD core plasma biomarkers in the Chinese Han community population. Previous clinical-based studies [50–52] have reported the potential of plasma biomarkers to identify CI individuals or predict cognitive decline in the Chinese Han population. In the present study, we recruited

a large Chinese Han population from the community in South China to define the cutoffs for plasma $A\beta_{42}/A\beta_{40}$ and plasma p-Tau$_{181}$ by comparing a large dataset of $A\beta$ PET negative CU individuals and $A\beta$ PET positive CI individuals. Consistent with the previous studies [36–40], one of the key findings in the present study was that plasma A+/T+individuals, defined by plasma $A\beta_{42}/A\beta_{40}$ and plasma p-Tau$_{181}$, showed the highest levels of astrocyte reactivity, $A\beta$ plaque, tau tangle, axonal degeneration, hippocampal atrophy, and cortical thinning. This supports the feasibility of using plasma $A\beta_{42}/A\beta_{40}$ and plasma p-Tau$_{181}$ to detect AD in the Chinese community older population. Compared to the plasma A-/T- group, plasma A+/T- individuals have higher plasma GFAP concentrations, whereas plasma A-/T+individuals had more $A\beta$ plaques. This indicates that plasma A+/T- individuals may exhibit astrocyte reactivity, whereas plasma A-/T+individuals may have early alternations in $A\beta$

Fig. 6 Vertex-wise association of plasma $A\beta_{42}/A\beta_{40}$ and plasma p-Tau$_{181}$ with cortical thickness images. Vertex-wise association of cortical thickness images with **(A-C)** plasma $A\beta_{42}/A\beta_{40}$ and **(D-F)** plasma p-Tau$_{181}$ in the whole cohort, individuals with plasma p-Tau$_{181}$ or plasma GFAP > Median and < Median. The plasma $A\beta_{42}/A\beta_{40}$ results were shown with an uncorrected voxel threshold of $p < 0.001$. For plasma p-Tau$_{181}$, the results were presented using an uncorrected voxel threshold of $p < 0.001$ with family-wise error corrected $p < 0.05$ at the cluster level, and the statistical results were overlaid onto inflated cortical surfaces. Notably, Plasma p-Tau$_{181}$ and plasma GFAP were $\log_{10}$ transferred before they were used in the general linear models

plaques rather than belong to the primary age-related tauopathy (PART) [53]. Consistent with our findings, one recent study [54] did not find significant increases in plasma p-Tau concentrations in individuals with PART defined by autopsy data. The cutoff of 0.0609 for the plasma $A\beta_{42}/A\beta_{40}$ ratio defined in the present study was comparable with the previously reported value with the autopsy data as the standard based on the European population [55]. Notably, the cutoff of 2.418 for plasma p-Tau181 was much more lenient than the value of 3.962 defined for the European population [55]. The different types of pre-analytical procedure [56], analytical [57], and real-world community studies [58] may explain the discrepancy. Future studies with larger and independent datasets in the Chinese Han community population are essential to validate the thresholds of plasma $A\beta_{42}/A\beta_{40}$ and plasma p-Tau$_{181}$ defined in the present study.

The regression findings were also consistent with the dichotomous analyses. Specifically, lower plasma $A\beta_{42}/A\beta_{40}$ was correlated with higher plasma GFAP concentrations and $A\beta$ plaques, while higher plasma p-Tau$_{181}$ was related to higher plasma GFAP concentration, $A\beta$ plaque, tau tangle, plasma NfL concentration, and more hippocampal atrophy. This further supports that plasma p-Tau$_{181}$ may be more closely linked to AD pathological changes than plasma $A\beta_{42}/A\beta_{40}$. In line with our findings, the BIOFINDER group [59] reported that plasma $A\beta_{42}/A\beta_{40}$ predicted longitudinal $A\beta$ accumulation, while higher plasma p-Tau$_{217}$ concentrations were associated with longitudinal tau accumulation. Besides, the Mayo group [36] noted that both plasma $A\beta_{42}/A\beta_{40}$ and plasma p-Tau$_{181}$ may be related to cortical $A\beta$ burden, with plasma p-Tau$_{181}$ showing the most improved discrimination of cortical tau tangles. Furthermore, lower plasma

$A\beta_{42}/A\beta_{40}$ and higher plasma p-Tau$_{181}$ had a marginal synergistic effect in predicting higher Aβ plaques, where individuals with high (>Median) plasma p-Tau$_{181}$ concentrations showed a stronger association with Aβ PET than those with low (<Median) concentrations. Together, these findings support the recommendation of staging AD biologically using both plasma $A\beta_{42}/A\beta_{40}$ and plasma p-Tau$_{181}$ biomarkers rather than plasma $A\beta_{42}/A\beta_{40}$ alone, as proposed by the NIA-AA revised clinical criteria for AD at AAIC 2023.

Previous literature [30, 31, 41–43] suggested plasma GFAP may be an early AD biomarker. One very recent study [29] demonstrated that plasma GFAP concentrations may modulate the relation between Aβ and tau in preclinical AD. Pelkmans and colleagues [44] also found that plasma GFAP may mediate the association between soluble and insoluble Aβ pathology in CU individuals. In the present study, we further demonstrated that the astrocyte reactivity measured by plasma GFAP significantly influences the association between plasma $A\beta_{42}/A\beta_{40}$ and plasma p-Tau$_{181}$ and their relations with the downstream events of AD, including AD-signature cortical tau aggregation and cortical thinning. Specifically, lower plasma $A\beta_{42}/A\beta_{40}$ was correlated with higher plasma p-Tau$_{181}$ concentrations and lower temporal-metaROI cortical thickness only in the presence of high astrocyte reactivity reflected by plasma GFAP. The plasma p-Tau$_{181}$-related higher cortical tau tangle aggregation and lower temporal-metaROI cortical thinning were more robust among individuals with high plasma GFAP concentrations than those with low plasma GFAP concentrations. Both higher plasma p-Tau$_{181}$ and plasma GFAP concentrations were related to higher plasma NfL concentrations, but no interaction was observed. Notably, higher plasma GFAP concentrations were unrelated to more cortical Aβ plaque accumulation or hippocampal atrophy, nor did they influence the association of plasma $A\beta_{42}/A\beta_{40}$ and plasma p-Tau$_{181}$ with cortical Aβ plaque accumulation or hippocampal atrophy. Together, these results suggest that the inflammation (I) biomarker plasma GFAP may play a cortical role in tau aggregation and cortical thinning in addition to plasma A/T biomarkers.

Consistent with previous findings [2, 60], we found a strong age effect in astrocyte activity measured by plasma GFAP, axonal degeneration measured by plasma NfL, and hippocampal atrophy. In contrast, no significant association with age was found in AD-signature cortical Aβ plaque accumulation, tau tangle aggregation, and cortical thinning. These findings suggest that Aβ PET, tau PET, and temporal-metaROI cortical thickness may be more relevant to AD pathological changes rather than the normal aging process. Additionally, we found females had more astrocyte reactivity but less axonal degeneration than males. Consequently, the age effect and sex

difference in plasma GFAP and plasma NfL concentrations should be considered when evaluating AD-related astrocyte reactivity and axonal degeneration. Consistent with previous findings, the *APOE-ε4* carriers showed higher cortical Aβ deposition [61] and less cortical thinning [62] than the *APOE-ε4* non-carriers.

In this study, we defined the community-useful thresholds for plasma $A\beta_{42}/A\beta_{40}$ and p-Tau$_{181}$ and evaluated their feasibility in identifying individuals with a high risk of AD based on Aβ PET, tau PET, and MRI image data in a large community-based Chinese aging cohort. Furthermore, this study demonstrated the critical role of astrocyte reactivity in AD progression, particularly in tau aggregation and cortical thinning in AD-signature cortical regions. This supports the usefulness of inflammation (I) biomarkers (such as plasma GFAP) to establish a more accurate diagnosis scheme in the clinic but also provides novel insights into understanding how astrocyte reactivity affects the cortical tau aggregation and cortical thinning in AD. However, all the analyses in this study were conducted based on cross-sectional data, and these findings are correlational in nature. Thus, this study does not establish plasma $A\beta_{42}/A\beta_{40}$, plasma p-Tau$_{181}$, or plasma GFAP as causal factors. All we can be sure of is that plasma GFAP seems to have a strong influence on elevated tau aggregation and cortical thinning in AD-signature cortical regions. Additionally, YKL40 may also be an astrocyte-related biomarker, which appears to be related to pathological AD changes in the late stage [44, 63]. Thus, further investigation is critical to confirm the influence of other astrocyte biomarkers in AD progression. Notably, the findings that higher plasma GFAP concentrations may be related to more plasma p-Tau181-related tau tangle aggregation should be validated using an independent cohort with a larger sample size in the future. Finally, the longitudinal data of plasma biomarkers, Aβ PET, tau PET, and MRI images are essential to validate all the cross-sectional findings in the present study.

Conclusions

In summary, this study established the thresholds of plasma $A\beta_{42}/A\beta_{40}$ and plasma p-Tau$_{181}$ measured by the Sioma platform and revealed the biological staging of AD scheme using plasma biomarkers in a Chinese community-based aging cohort. Plasma $A\beta_{42}/A\beta_{40}$ positive and plasma p-Tau$_{181}$ positive (A+/T+) individuals showed significant evidence of cortical Aβ deposition, tau aggregation, hippocampal atrophy, and cortical thinning. The first-defined community useful thresholds of plasma $A\beta_{42}/A\beta_{40}$ and plasma p-Tau$_{181}$ in the older Chinese Han population offer a significant reference for early AD diagnosis in China, although more validation is still essential. The astrocyte reactivity reflected by plasma GFAP may be a promising "I" biomarker, augmenting the progression

of A+/T+individuals defined by plasma $A\beta_{42}/A\beta_{40}$ and plasma p-Tau$_{181}$. These findings indicate that the A/T/I profiles may provide more comprehensive information for selecting high AD-risk individuals for clinical trials and highlight the importance of targeting reactive astrogliosis to prevent AD progression.

Abbreviations

Aβ	β-amyloid
A+	Aβ positive
APOE	Apolipoprotein E
β$_{std}$	standardizedβ
CI	Cognitive impaired
ci	confidence interval
CSF	cerebrospinal fluid
CU	cognitively unimpaired
FSP	[18 F]D3FSP
FTP	[18 F]-flortaucipir
FWE	family-wise error
GFAP	Glial fibrillary acidic protein
GHABS	Greater-Bay-Area Healthy Aging Brain Study
IQR	Interquartile range
MCI	Mild cognitive impairment
NfL	Neurofilament light
p-Tau	Phosphorylated tau
rHCV	residual hippocampal volume
ROC	Receiver operating characteristic curve
ROI	Region of interest
SCD	Subjective cognitive decline
SUVR	Standardized uptake value ratio
T+	Tau positive

Supplementary Information

The online version contains supplementary material available at https://doi.org/10.1186/s13024-024-00750-8.

Supplementary Material 1

Supplementary Material 2

Declarations

Ethics approval and consent to participate
All procedures performed in studies involving human participants were in accordance with the ethical standards of the institutional and/or national research committee and with the principles of the 1964 Declaration of Helsinki and its later amendments or comparable ethical standards. Formed written consent was obtained from all GHABS participants.

Competing interests
The authors report no competing interests.

Author details
[1]Institute of Biomedical Engineering, Shenzhen Bay Laboratory, No.5 Kelian Road, Shenzhen 518132, China
[2]Institute of Biomedical Engineering, Peking University Shenzhen Graduate School, Shenzhen 518055, China
[3]Department of Neurology, Xuanwu Hospital of Capital Medical University, #45 Changchun Street, Xicheng District, Beijing 100053, China
[4]Department of Nuclear Medicine, The First Affiliated Hospital, Guangzhou Medical University, Guangzhou 510120, China
[5]Department of Neurology, Peking University Shenzhen Hospital, Shenzhen 518000, China
[6]Neurology Medicine Center, The Seventh Affiliated Hospital, Sun Yat-sen University, Shenzhen 518000, China
[7]Department of Neurology, Shenzhen Guangming District People's Hospital, Shenzhen 518107, China
[8]Department of Medical Imaging, Shenzhen Guangming District People's Hospital, Shenzhen 518106, China
[9]Department of Nuclear Medicine, Guangdong Hospital of Traditional Chinese Medicine, Guangzhou 510120, China
[10]Institute of Cancer Research, Shenzhen Bay Laboratory, Shenzhen 518132, China
[11]School of Biomedical Engineering, Hainan University, Haikou 570228, China
[12]Center of Alzheimer's Disease, Beijing Institute for Brain Disorders, Beijing 100053, China
[13]National Clinical Research Center for Geriatric Diseases, Beijing 100053, China
[14]Department of Radiology and Nuclear Medicine, Xuanwu Hospital, Capital Medical University, #45 Changchun Street, Xicheng District, Beijing 100053, China

References
1. Guo T, Shaw LM, Trojanowski JQ, Jagust WJ, Landau SM. Association of CSF Aβ, amyloid PET, and cognition in cognitively unimpaired elderly adults. Neurology. 2020;95:e2075–85.
2. Shi D, Xie S, Li A, Wang Q, Guo H, Han Y, et al. APOE-ε4 modulates the association among plasma Aβ42/Aβ40, vascular diseases, neurodegeneration and cognitive decline in non-demented elderly adults. Transl Psychiatry. 2022;12:128.
3. Cai Y, Shi D, Lan G, Chen L, Jiang Y, Zhou L, et al. Association of β-Amyloid, Microglial activation, cortical thickness, and metabolism in older adults without dementia. Neurology. 2024;102:e209205.
4. Guo T, Landau SM, Jagust WJ. Detecting earlier stages of amyloid deposition using PET in cognitively normal elderly adults. Neurology. 2020;94:e1512–24.
5. Guo T, Dukart J, Brendel M, Rominger A, Grimmer T, Yakushev I. Rate of β-amyloid accumulation varies with baseline amyloid burden: implications for anti-amyloid drug trials. Alzheimer's Dement. 2018;14:1387–96.

6. Guo T, Korman D, La Joie R, Shaw LM, Trojanowski JQ, Jagust WJ, et al. Normalization of CSF pTau measurement by Aβ40 improves its performance as a biomarker of Alzheimer's disease. Alzheimers Res Ther. 2020;12:97.

7. Cai Y, Du J, Li A, Zhu Y, Xu L, Sun K, et al. Initial levels of β-amyloid and tau deposition have distinct effects on longitudinal tau accumulation in Alzheimer's disease. Alzheimers Res Ther. 2023;15:30.

8. Jiang C, Wang Q, Xie S, Chen Z, Fu L, Peng Q et al. β-Amyloid discordance of cerebrospinal fluid and positron emission tomography imaging shows distinct spatial tau patterns. Brain Commun. 2022;4.

9. Guo T, Korman D, Baker SL, Landau SM, Jagust WJ. Longitudinal cognitive and biomarker measurements support a unidirectional pathway in Alzheimer's Disease Pathophysiology. Biol Psychiatry. 2021;89:786–94.

10. Lan G, Cai Y, Li A, Liu Z, Ma S, Guo T. Association of Presynaptic Loss with Alzheimer's Disease and Cognitive decline. Ann Neurol. 2022;92:1001–15.

11. Lan G, Li A, Liu Z, Ma S, Guo T. Presynaptic membrane protein dysfunction occurs prior to neurodegeneration and predicts faster cognitive decline. Alzheimer's Dement. 2023;19:2408–19.

12. Patani R, Hardingham GE, Liddelow SA. Functional roles of reactive astrocytes in neuroinflammation and neurodegeneration. Nat Rev Neurol. 2023;19:395–409.

13. Guo T, Brendel M, Grimmer T, Rominger A, Yakushev I. Predicting Regional Pattern of Longitudinal β-Amyloid Accumulation by Baseline PET. J Nucl Med. 2017;58:639–45.

14. Altomare D, de Wilde A, Ossenkoppele R, Pelkmans W, Bouwman F, Groot C, et al. Applying the ATN scheme in a memory clinic population: the ABIDE project. Neurology. 2019;93:e1635–46.

15. Soldan A, Pettigrew C, Fagan AM, Schindler SE, Moghekar A, Fowler C, et al. ATN profiles among cognitively normal individuals and longitudinal cognitive outcomes. Neurology. 2019;92:e1567–79.

16. Strikwerda-Brown C, Hobbs DA, Gonneaud J, St-Onge F, Binette AP, Ozlen H, et al. Association of Elevated Amyloid and tau Positron Emission Tomography Signal with Near-Term Development of Alzheimer Disease symptoms in older adults without cognitive impairment. JAMA Neurol. 2022;79:975.

17. Ossenkoppele R, Pichet Binette A, Groot C, Smith R, Strandberg O, Palmqvist S, et al. Amyloid and tau PET-positive cognitively unimpaired individuals are at high risk for future cognitive decline. Nat Med. 2022;28:2381–7.

18. Jack CR, Wiste HJ, Therneau TM, Weigand SD, Knopman DS, Mielke MM, et al. Associations of amyloid, Tau, and Neurodegeneration Biomarker profiles with Rates of memory decline among individuals without dementia. JAMA. 2019;321:2316.

19. Nakamura A, Kaneko N, Villemagne VL, Kato T, Doecke J, Doré V, et al. High performance plasma amyloid-β biomarkers for Alzheimer's disease. Nature. 2018;554:249–54.

20. Schindler SE, Bollinger JG, Ovod V, Mawuenyega KG, Li Y, Gordon BA, et al. High-precision plasma β-amyloid 42/40 predicts current and future brain amyloidosis. Neurology. 2019;93:e1647–59.

21. Hirtz C, Busto GU, Bennys K, Kindermans J, Navucet S, Tiers L, et al. Comparison of ultrasensitive and mass spectrometry quantification of blood-based amyloid biomarkers for Alzheimer's disease diagnosis in a memory clinic cohort. Alzheimers Res Ther. 2023;15:34.

22. Palmqvist S, Janelidze S, Quiroz YT, Zetterberg H, Lopera F, Stomrud E, et al. Discriminative accuracy of plasma Phospho-tau217 for Alzheimer Disease vs Other Neurodegenerative disorders. JAMA. 2020;324:772.

23. Thijssen EH, La Joie R, Wolf A, Strom A, Wang P, Iaccarino L, et al. Diagnostic value of plasma phosphorylated tau181 in Alzheimer's disease and frontotemporal lobar degeneration. Nat Med. 2020;26:387–97.

24. Karikari TK, Pascoal TA, Ashton NJ, Janelidze S, Benedet AL, Rodriguez JL, et al. Blood phosphorylated tau 181 as a biomarker for Alzheimer's disease: a diagnostic performance and prediction modelling study using data from four prospective cohorts. Lancet Neurol. 2020;19:422–33.

25. Janelidze S, Mattsson N, Palmqvist S, Smith R, Beach TG, Serrano GE, et al. Plasma P-tau181 in Alzheimer's disease: relationship to other biomarkers, differential diagnosis, neuropathology and longitudinal progression to Alzheimer's dementia. Nat Med. 2020;26:379–86.

26. Thijssen EH, La Joie R, Strom A, Fonseca C, Iaccarino L, Wolf A, et al. Plasma phosphorylated tau 217 and phosphorylated tau 181 as biomarkers in Alzheimer's disease and frontotemporal lobar degeneration: a retrospective diagnostic performance study. Lancet Neurol. 2021;20:739–52.

27. Ashton NJ, Pascoal TA, Karikari TK, Benedet AL, Lantero-Rodriguez J, Brinkmalm G, et al. Plasma p-tau231: a new biomarker for incipient Alzheimer's disease pathology. Acta Neuropathol. 2021;141:709–24.

28. Mielke MM, Dage JL, Frank RD, Algeciras-Schimnich A, Knopman DS, Lowe VJ, et al. Performance of plasma phosphorylated tau 181 and 217 in the community. Nat Med. 2022;28:1398–405.

29. Bellaver B, Povala G, Ferreira PCL, Ferrari-Souza JP, Leffa DT, Lussier FZ, et al. Astrocyte reactivity influences amyloid-β effects on tau pathology in preclinical Alzheimer's disease. Nat Med. 2023;29:1775–81.

30. Chatterjee P, Vermunt L, Gordon BA, Pedrini S, Boonkamp L, Armstrong NJ, et al. Plasma glial fibrillary acidic protein in autosomal dominant Alzheimer's disease: associations with Aβ-PET, neurodegeneration, and cognition. Alzheimer's Dement. 2023;19:2790–804.

31. Stocker H, Beyer L, Perna L, Rujescu D, Holleczek B, Beyreuther K, et al. Association of plasma biomarkers, p-tau181, glial fibrillary acidic protein, and neurofilament light, with intermediate and long-term clinical Alzheimer's disease risk: results from a prospective cohort followed over 17 years. Alzheimer's Dement. 2023;19:25–35.

32. Guzmán-Vélez E, Zetterberg H, Fox-Fuller JT, Vila-Castelar C, Sanchez JS, Baena A, et al. Associations between plasma neurofilament light, in vivo brain pathology, and cognition in non-demented individuals with autosomal-dominant Alzheimer's disease. Alzheimer's Dement. 2021;17:813–21.

33. Bangen KJ, Thomas KR, Weigand AJ, Edmonds EC, Clark AL, Solders S, et al. Elevated plasma neurofilament light predicts a faster rate of cognitive decline over 5 years in participants with objectively-defined subtle cognitive decline and MCI. Alzheimer's Dement. 2021;17:1756–62.

34. Blennow K, Galasko D, Perneczky R, Quevenco F, van der Flier WM, Akinwonmi A et al. The potential clinical value of plasma biomarkers in Alzheimer's disease. Alzheimer's Dement. 2023;1–12.

35. Hampel H, Hu Y, Cummings J, Mattke S, Iwatsubo T, Nakamura A, et al. Blood-based biomarkers for Alzheimer's disease: current state and future use in a transformed global healthcare landscape. Neuron. 2023;111:2781–99.

36. Jack CR, Wiste HJ, Algeciras-Schimnich A, Figdore DJ, Schwarz CG, Lowe VJ, et al. Predicting amyloid PET and tau PET stages with plasma biomarkers. Brain. 2023;146:2029–44.

37. Meyer P, Ashton NJ, Karikari TK, Strikwerda-Brown C, Köbe T, Gonneaud J, et al. Plasma p-tau231, p-tau181, PET biomarkers, and cognitive change in older adults. Ann Neurol. 2022;91:548–60.

38. Janelidze S, Palmqvist S, Leuzy A, Stomrud E, Verberk IMW, Zetterberg H, et al. Detecting amyloid positivity in early Alzheimer's disease using combinations of plasma Aβ42/Aβ40 and p-tau. Alzheimer's Dement. 2022;18:283–93.

39. Xiao Z, Wu W, Ma X, Liang X, Lu J, Zheng L, et al. Plasma Aβ42/Aβ40 and p-tau181 Predict Long-Term Clinical Progression in a cohort with amnestic mild cognitive impairment. Clin Chem. 2022;68:1552–63.

40. Chatterjee P, Pedrini S, Doecke JD, Thota R, Villemagne VL, Doré V, et al. Plasma Aβ42/40 ratio, p-tau181, GFAP, and NfL across the Alzheimer's disease continuum: a cross-sectional and longitudinal study in the AIBL cohort. Alzheimer's Dement. 2023;19:1117–34.

41. Beyer L, Stocker H, Rujescu D, Holleczek B, Stockmann J, Nabers A, et al. Amyloid-beta misfolding and GFAP predict risk of clinical Alzheimer's disease diagnosis within 17 years. Alzheimer's Dement. 2023;19:1020–8.

42. Guo Y, Shen X-N, Wang H-F, Chen S-D, Zhang Y-R, Chen S-F, et al. The dynamics of plasma biomarkers across the Alzheimer's continuum. Alzheimers Res Ther. 2023;15:31.

43. Pereira JB, Janelidze S, Smith R, Mattsson-Carlgren N, Palmqvist S, Teunissen CE, et al. Plasma GFAP is an early marker of amyloid-β but not tau pathology in Alzheimer's disease. Brain. 2021;144:3505–16.

44. Pelkmans W, Shekari M, Brugulat-Serrat A, Sánchez-Benavides G, Minguillón C, Fauria K et al. Astrocyte biomarkers GFAP and YKL-40 mediate early Alzheimer's disease progression. Alzheimer's Dement. 2023;1–11.

45. Liu Z, Shi D, Cai Y, Li A, Lan G, Sun P, et al. Pathophysiology characterization of Alzheimer's disease in South China's aging population: for the Greater-Bay-Area healthy aging brain study (GHABS). Alzheimers Res Ther. 2024;16:84.

46. Petersen RC, Aisen PS, Beckett LA, Donohue MC, Gamst AC, Harvey DJ, et al. Alzheimer's Disease Neuroimaging Initiative (ADNI): clinical characterization. Neurology. 2010;74:201–9.

47. Jack CR, Wiste HJ, Weigand SD, Therneau TM, Lowe VJ, Knopman DS, et al. Defining imaging biomarker cut points for brain aging and Alzheimer's disease. Alzheimer's Dement. 2017;13:205–16.

48. Li A, Zhao R, Zhang M, Sun P, Cai Y, Zhu L et al. [18F]-D3FSP β-amyloid PET imaging in older adults and alzheimer's disease. Eur J Nucl Med Mol Imaging. 2024.

49. Fleisher AS, Pontecorvo MJ, Devous MD, Lu M, Arora AK, Truocchio SP, et al. Positron Emission Tomography Imaging with [18 F]flortaucipir and

Postmortem Assessment of Alzheimer Disease Neuropathologic Changes. JAMA Neurol. 2020;77:829.

50. Shen X, Huang S-Y, Cui M, Zhao Q, Guo Y, Huang Y, et al. Plasma glial fibrillary acidic protein in the Alzheimer Disease Continuum: relationship to other biomarkers, Differential diagnosis, and prediction of clinical progression. Clin Chem. 2023;69:411–21.

51. Wu X, Xiao Z, Yi J, Ding S, Gu H, Wu W, et al. Development of a plasma Biomarker Diagnostic Model incorporating Ultrasensitive Digital Immunoassay as a screening strategy for Alzheimer Disease in a Chinese Population. Clin Chem. 2021;67:1628–39.

52. Gao F, Lv X, Dai L, Wang Q, Wang P, Cheng Z, et al. A combination model of AD biomarkers revealed by machine learning precisely predicts Alzheimer's dementia: China Aging and Neurodegenerative Initiative (CANDI) study. Alzheimer's Dement. 2023;19:749–60.

53. Crary JF, Trojanowski JQ, Schneider JA, Abisambra JF, Abner EL, Alafuzoff I, et al. Primary age-related tauopathy (PART): a common pathology associated with human aging. Acta Neuropathol. 2014;128:755–66.

54. Montoliu L, Michael G, Yhang E, Tripodis Y, Sconzo D, Ally M. Optimal blood tau species for the detection of Alzheimer 's disease neuropathology: an immunoprecipitation mass spectrometry and autopsy study. Acta Neuropathol. 2024.

55. Smirnov DS, Ashton NJ, Blennow K, Zetterberg H, Simrén J, Lantero-Rodriguez J, et al. Plasma biomarkers for Alzheimer's Disease in relation to neuropathology and cognitive change. Acta Neuropathol. 2022;143:487–503.

56. Verberk IMW, Misdorp EO, Koelewijn J, Ball AJ, Blennow K, Dage JL, et al. Characterization of pre-analytical sample handling effects on a panel of Alzheimer's disease–related blood-based biomarkers: results from the standardization of Alzheimer's blood biomarkers (SABB) working group. Alzheimer's Dement. 2022;18:1484–97.

57. Hansson O, Edelmayer RM, Boxer AL, Carrillo MC, Mielke MM, Rabinovici GD, et al. The Alzheimer's Association appropriate use recommendations for blood biomarkers in Alzheimer's disease. Alzheimer's Dement. 2022;18:2669–86.

58. Huber H, Ashton NJ, Schieren A, Montoliu-Gaya L, Molfetta G, Di, Brum WS et al. Levels of Alzheimer's disease blood biomarkers are altered after food intake—A pilot intervention study in healthy adults. Alzheimer's Dement. 2023;1–10.

59. Pereira JB, Janelidze S, Stomrud E, Palmqvist S, van Westen D, Dage JL, et al. Plasma markers predict changes in amyloid, tau, atrophy and cognition in non-demented subjects. Brain. 2021;144:2826–36.

60. Chatterjee P, Pedrini S, Ashton NJ, Tegg M, Goozee K, Singh AK, et al. Diagnostic and prognostic plasma biomarkers for preclinical Alzheimer's disease. Alzheimer's Dement. 2022;18:1141–54.

61. Gonneaud J, Arenaza-Urquijo EM, Fouquet M, Perrotin A, Fradin S, De La Sayette V, et al. Relative effect of APOE ϵ4 on neuroimaging biomarker changes across the lifespan. Neurology. 2016;87:1696–703.

62. Mattsson N, Ossenkoppele R, Smith R, Strandberg O, Ohlsson T, Jögi J, et al. Greater tau load and reduced cortical thickness in APOE ε4-negative Alzheimer's disease: a cohort study. Alzheimers Res Ther. 2018;10:77.

63. Ferrari-Souza JP, Ferreira PCL, Bellaver B, Tissot C, Wang Y-T, Leffa DT, et al. Astrocyte biomarker signatures of amyloid-β and tau pathologies in Alzheimer's disease. Mol Psychiatry. 2022;27:4781–9.

Publisher's Note